

Band-aid for information loss from black holes

Werner Israel and Zinkoo Yun¹

Department of physics and astronomy University of Victoria
Victoria, BC, Canada V8W 3P6

Abstract

We summarize, simplify and extend recent work showing that small deviations from exact thermality in Hawking radiation, first uncovered by Kraus and Wilczek, have the capacity to carry off the maximum information content of a black hole. This goes a considerable way toward resolving a long-standing “information loss paradox.”

¹Israel:israel@uvic.ca
Yun:semiro@uvic.ca

1 Introduction

Hawking’s dramatic 1974 announcement that black holes evaporate thermally has led to a much-discussed paradox. If, as indicated by Hawking’s semi-classical analysis, the radiation spectrum is exactly thermal (thus fully characterized by just a single parameter, temperature), the consequent loss of information violates a basic quantum principle, unitarity. A number of resolutions of this puzzle have been proposed, some of them are quite radical [1].

A conservative option, developed from 1994 by Frank Wilczek and his collaborators [2], is that back-reaction of the emissions on the geometry and thermal properties of the hole could result in information-carrying departures from thermality. Specifically, emission of each discrete quantum is attended by a jump of Hawking temperature, hence no longer definable by a single parameter. Correlations carried by the resulting deviations from thermality, while individually small, could build up to a substantial information capacity over the course of the hole’s lifetime.

Although earlier studies cast doubt on this possibility [3], recent work by Zhang et al [4] has given it credence. They concluded that up to $\exp S_{BH}$ bits of information can be carried off in the correlations, which can include all of the information in the hole if, as seems reasonable, the Bekenstein-Hawking entropy $S_{BH} = A/4$ is a measure of the hole’s *information capacity*, in the sense that $\exp S_{BH}$ is the maximum number of bits that can be accommodated in a black hole formed by an astrophysical collapse.

Kraus and Wilczek’s key result [2] was their arithmetic-mean prescription (AMP, cf (4.13) below) for the effective action (including back-reaction) of a massive particle (modelled as a spherical shell in the s-wave approximation) tunneling out of a spherical black hole. Their analysis was encumbered by use of the intricate machinery of spherisymmetric Hamiltonian gravity and required a dozen pages of closely reasoned argument even for the simplest example of uncharged (Schwarzschild) evaporation.

The much simpler and more transparent treatment introduced here calls upon the general-relativistic dynamics of thin shells, together with the analytic properties of Schwarzschild’s time co-ordinate t over the extended Kruskal manifold, and occupies just a few lines (Sec. 4). Moreover, this extends immediately to charged evaporation and brings new aspects of the problem into focus – breakdown of AMP when interactions with nongravitational forces are introduced, the extremal (zero-temperature) limit and the possibility of black hole remnants. These aspects are further discussed (but not fully resolved) in Sec. 4, and the need for further work emphasized.

By way of introduction to this somewhat novel treatment of the black hole tunneling problem, Sec. 3 rederives the classic Schwinger formula for charged pair creation by an electric field, using the same (essentially geometrical) approach. Comparison is instructive, revealing both the resemblance and at least one sharp difference between the two cases.

Sec. 5 briefly reviews the key question on which the current literature makes a confused impression – does Hawking radiation with Kraus-Wilczek deviations from thermality have information-holding correlations? – and reaffirms the positive answer given by Zhang et al [4]. Sec. 6 concludes the paper with some open questions.

2 Tunneling

“Tunneling” (or “barrier penetration”) is the term commonly used for energy-conserving quantum transitions that are classically forbidden. In such cases, a path-integral evaluation of the transition amplitude is hampered by the fact that the sum-over-paths is not dominated by any single(real) path. The familiar remedy is analytic continuation of the time coordinate to pure imaginary values. In the resulting Euclidean-signature spacetime a classical tunneling route often exists and dominates the sum-over-paths. The procedure is analogous to the steepest-descent method for evaluating a real definite integral by diverting the integration contour through a saddle point in the complex plane. (cf [8])

Equivalently, one can set out from the time-independent Schrödinger equation for a fixed energy. The ansatz $\psi = \exp iW$ yields the Hamilton-Jacobi equation for W in WKB approximation. This identifies W as the Jacobi action or Hamilton’s characteristic function:

$$W = \int (L + H) dt. \quad (2.1)$$

Among orbits of given energy between two given configurations, W is minimized by the classical orbit. For configurations separated by a barrier, but connectable by a classical tunneling orbit in imaginary time, W becomes complex and gives a tunneling probability

$$P = \psi\psi^* = \exp(-2\text{Im } W) \quad (2.2)$$

in lowest-order approximation. (For more detatails, see e.g. [9])

Equation (2.2) has rather general validity and is readily applicable in situations where a tunneling path can be clearly defined, as in the case of a particle. For a field, a reduction procedure is needed to describe the tunneling of a 1-particle excitation. In an s-wave approximation on a spherical background (e.g. a spherical black hole) the excitation can be modelled as a spherical shell. (The reduction is spelled out in some detail by Kraus and Wilczek [10] for the special case of a charged scalar field propagating on the classical background of a radial electric field.) When we treat tunneling out of a spherical black hole in Sec.4 we shall circumvent this rather elaborate reduction by inserting into (2.1) the natural and simplest material action that is minimized by the classical orbit of the shell.

3 Pair creation in a uniform electric field revisited

The intuitive picture of tunneling out of a black hole suggested by the Parikh-Wilczek calculation [2] is at first glance very different from the familiar one of charged-pair creation by a strong electric field. There is no black hole counterpart to the finite-width potential barrier that separates the oppositely charged pair. In a black hole the barrier is a causal one – the light cone that forms the future horizon. There are nonetheless strong resemblances between the two pictures. In this section we shall briefly re-derive Schwinger’s results [5] to leading order in a geometrical way that points up the resemblance as well as highlighting an essential difference.

We consider a uniform electric field \mathcal{E} directed along the positive x-axis of Minkowski space-time. The energy of a point charge e moving along the x-axis is

$$E = m\gamma - e\mathcal{E}x, \quad \gamma = \frac{1}{\sqrt{1-v^2}} \quad (3.1)$$

Intuitively, a virtual pair (e, m) and $(-e, m)$ located at $x_+(t)$ and $x_-(t)$ can extract enough energy ($\geq 2m$) to emerge as a real pair if they happen to reach a minimum separation determined by

$$x_+(0) = -x_-(0) = \frac{1}{a}, \quad a = \frac{e\mathcal{E}}{m} \quad (3.2)$$

with a convenient choice of origin. Assuming (3.2) as initial condition, the equation of motion

$$\frac{dp}{dt} = e\mathcal{E}, \quad p = m\gamma \frac{dx}{dt} \quad (3.3)$$

integrates to give the hyperbolic path (parametrized by proper time τ)

$$ax = \cosh a\tau, \quad at = \sinh a\tau \quad (3.4)$$

for the newly created positive charge e , with e replaced by $-e$ for its partner. The two orbits are shown as CD and AB in Figure 1.

It is straightforward to recast this picture of pair creation as a one-particle history. The particle's orbit may be traced through three stages (AB, BC and CD in Fig 1), in each of which the orbital equation is given by analytic extension of (3.2) in the complex τ -plane, $\tau = \tau_R + i\tau_I$.

In the first stage AB, given by

$$-\infty \leq \tau_R \leq 0, \quad a\tau_I = \pi, \quad (3.5)$$

so that (3.4) becomes

$$ax = -\cosh a\tau_R, \quad at = -\sinh a\tau_R, \quad (3.6)$$

the particle enters from the left, moving backward in Lorentz time t , and is slowed by the field (so that its effective charge/mass ratio at this stage is really $e/(-m)$) until it comes to momentary rest at B.

The second (tunneling) stage is an excursion into imaginary time

$$\tau = i\tau_I, \quad a\tau_I = \theta, \quad t = it_I \quad (3.7)$$

and imaginary momentum p . The orbit (3.4) is now the semicircle BC:

$$ax = \cos \theta, \quad at_I = \sin \theta \quad (\theta : \pi \rightarrow 0) \quad (3.8)$$

In the third stage CD, given by $0 \leq \tau \leq \infty$, the orbit has re-entered real time and (3.4) describes the conventional picture of a particle, with charge/mass ratio e/m , being accelerated to the right.

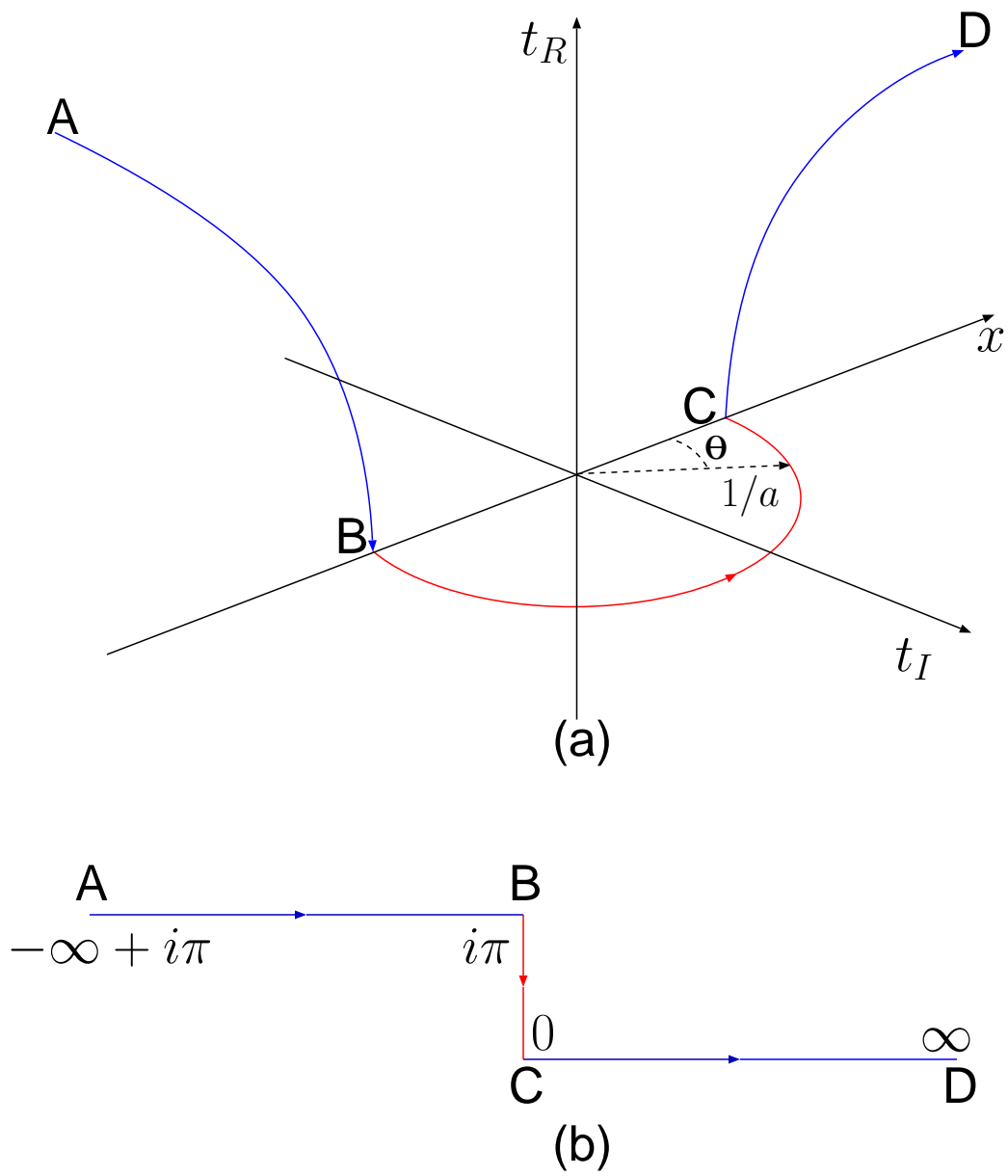


Figure 1: (a) Electron pair creation as tunneling. (b) March of $a\tau$

The whole sequence may be interpreted as representing a virtual charge e which has increased its effective mass from $-m$ to $+m$ by extracting energy $2m$ from the field during the tunneling phase.

From (3.1) and (3.4) it is easily checked directly that the total energy E is conserved and, moreover, vanishing for this virtual particle. Thus we do not need to distinguish between the Jacobi and Lagrange actions in this instance:

$$W = I = - \int m d\tau + \int e A_\alpha dx^\alpha = - \int (m d\tau + e \varphi dt) \quad (3.9)$$

Setting $\varphi = -\mathcal{E}x$ and recalling that $e\mathcal{E} = ma$, we easily obtain from (3.7) and (3.8) for the tunneling phase

$$W^{BC} = -\frac{im}{a} \int_\pi^0 \sin^2 \theta d\theta = \frac{i\pi m}{2a} \quad (3.10)$$

Hence the tunneling probability is

$$P = e^{-2\text{Im } W} = \exp\left(-\pi m^2/e\mathcal{E}\right) \quad (3.11)$$

in agreement with Schwinger's classic result [1].

Our treatment of gravitational tunneling in the following section will closely follow these lines, but with one key difference. In the electric tunneling phase BC, work done on the rest mass by the field reversed its sign from $-m$ to $+m$, or (equivalently) reversed the sense of proper time τ . The effect was a sign reversal of the inertial term $-\int m d\tau$ in the action (3.9), which was implemented by complexifying τ . In contrast, for a particle moving under gravity the gravitational force vanishes in its rest-frame by the equivalence principle and cannot affect its rest mass. Thus the inertial action and proper time remain real during the tunneling phase.

4 Tunneling out of a spherical black hole.

Figure 2 is a Kruskal map of an eternal black hole, partitioned by the two horizon sheets (at fixed θ, ϕ) into left, right, future and past sectors L, R, F and P. Our universe is taken to be the R-sector; In terms of this idealized eternal picture, the tunneling and evaporation of a particle can come about in two distinct ways.

4.1 L→R tunneling in an eternal black hole.

Energetically, the cheapest (hence most probable) tunneling route is to a configuration in which the emerging particle has no kinetic energy. So this mechanism treats transitions between static or momentarily static configurations on opposite sides of the horizon. A virtual particle (world line AB in Figure 2) starts from rest in sector L, enters a tunneling mode at B, then circulates in complex time around the semi-circle to C, whence it emerges in sector R as a real static particle. Meanwhile, the hole's mass and charge have been reduced,

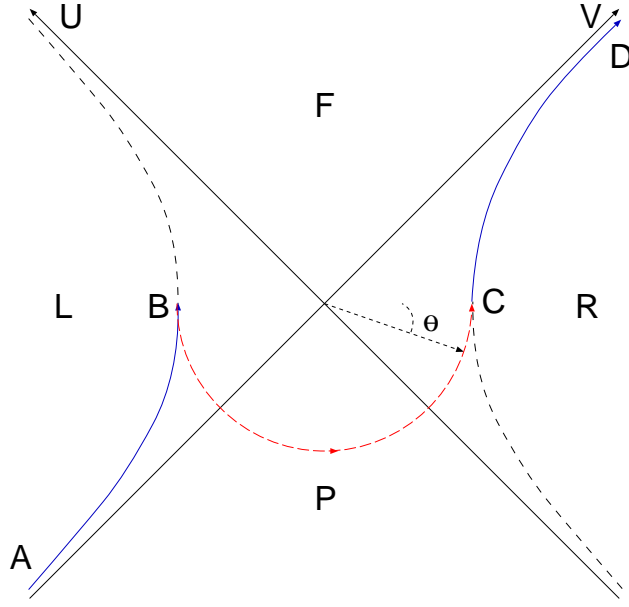


Figure 2: $L \rightarrow R$ tunneling in an eternal black hole

and the surface gravity κ correspondingly increased, by loss of this particle - from κ_L in sector L before the tunneling, to κ_R in sector R after the particle has escaped. This picture closely resembles the Schwinger tunneling picture of Figure 1.

Eternal black holes are not formed by real astrophysical collapse. The initial tunneling state in sector L has no real counterpart. So this tunneling model is further removed from reality than the picture of direct tunneling from F to R that we shall consider in the next section. However, it can be formulated completely and precisely, and allows effects of back-reaction to be easily accommodated. The extra stretch of the tunneling route from L into F en route to R adds no imaginary part to the action, since falling from L into F is classically allowable.

To fix notation, the spherical geometries that we consider in this section have metrics of the general form

$$ds^2 = \frac{dr^2}{f(r)} + r^2 d\Omega^2 - f(r) dt^2$$

This includes Schwarzschild and Reissner-Nordström black holes imbedded in flat, de Sitter or AdS backgrounds. At the horizon $f(r_0) = 0$ and the surface gravity is $\kappa = \frac{1}{2}f'(r_0)$ (assumed non vanishing).

Advanced and retarded Eddington-Finkelstein coordinates u, v are defined by

$$\begin{cases} du = dt - \frac{dr}{f(r)} \\ dv = dt + \frac{dr}{f(r)} \end{cases} \quad (4.1)$$

and the corresponding Kruskal coordinates U, V by

$$U = -e^{-\kappa u}, \quad V = e^{\kappa v}$$

In these coordinates, the metric is

$$ds^2 = \frac{f(r)}{\kappa^2 UV} dU dV + r^2(U, V) d\Omega^2$$

and is manifestly regular for all points (U, V) where $f(r)$ is regular, including the two horizon sheets $U = 0$ and $V = 0$.

Schwarzschild time t is initially defined only over the R-sector of the extended Kruskal manifold of Figure 2. It will be useful to extend it analytically to the full space in such a way that $e^{-i\omega t}$ is positive-frequency with respect to the globally regular times U and V . This requires that $e^{-i\omega t}$ be regular and bounded in the lower halves of the complex U and V planes. A definition which achieves this is

$$t = \frac{1}{2\kappa} \ln \frac{V}{U} \quad (4.2)$$

in which we have selected that branch of $\ln z$ which is regular on the lower-half z -plane, and real on the lower imaginary axis, so that its values, e.g for real x ,

$$\ln x \equiv \ln |x| + \frac{i\pi}{2} \epsilon(x) \quad (4.3)$$

are left-right symmetric. The imaginary constant thereby added to t in (4.2) does not affect time-differences in a given sector. Moreover, it ensures manifest CPT invariance of the analytically extended transition and tunneling amplitudes that we are about to derive, i.e., invariance under simultaneous reversal of t, U, V .

Schwarzschild time t is regular along the entire tunneling path ABCD (Fig 2) and the background geometry is static (apart from small back-reaction effects). It is therefore a suitable candidate to be complexified and used as the parameter for L→R tunneling.

In an s-wave approximation the tunneling (charged) particle is modeled as a spherical shell. According to (A.24) in Appendix A, the appropriate (Jacobi) action is

$$W = - \int M d\tau + \int E d\bar{t} \quad (4.4)$$

Here, M is the proper mass of the shell, τ its proper time and the bar in $\bar{t} = \frac{1}{2}(t_+ + t_-)$ an arithmetical average over the two geometries, $f_+(r)$ and $f_-(r)$ exterior and interior to the shell. Finally, E is the energy of the shell when it emerges from the tunneling phase at C. If the shell is uncharged, and with just enough energy to reach infinity, this is simply the Schwarzschild mass, $E = m_+ - m_-$. For a shell with charge $q = e_+ - e_-$ emerging from a charged hole, E is smaller than this by $\bar{c} \equiv q(e/r_H)$, the work done in lifting the shell from the horizon to infinity. Thus, generally,

$$E = m - q\bar{\Phi}_H \quad (4.5)$$

where Φ_H is the electric potential at the horizon. From (4.2),

$$\text{Im } t_B = -\frac{i\pi}{2\kappa_L}, \quad \text{Im } t_C = +\frac{i\pi}{2\kappa_R} \quad (4.6)$$

valid for t_+ , t_- and \bar{t} .

Thus, for an emission with Schwarzschild mass-energy E

$$\text{Im } W(E) = \text{Im} \int E d\bar{t} = E \text{Im} \int d\bar{t} \quad (4.7)$$

$$= \frac{\pi}{2} E \left(\frac{1}{\kappa_R} + \frac{1}{\kappa_L} \right) = E \pi \overline{\left(\frac{1}{\kappa} \right)} \quad (4.8)$$

stemming from the imaginary-time path BC. This agrees with the Parikh-Wilczek result [2] derived in Painlevé-Gullstrand coordinates. Hence the tunneling probability for emission of Schwarzschild mass-energy E from a charged black hole is, by (2.2),

$$P(E) = e^{-2\text{Im } W} = e^{-\beta(E)E}, \quad \beta \equiv \overline{\left(\frac{2\pi}{\kappa} \right)} \quad (4.9)$$

in which the effective Hawking temperature $T_H = 1/\beta$ is given as the harmonic mean of surface gravities κ_L and κ_R before and after emission.

The energy distribution (4.9) was first derived by Kraus and Wilczek [2] by a more elaborate route. Since β depends on E , (4.9) is no longer a simple Boltzmann exponential. As shown by Zhang et al [4] (and as we shall outline in Sec. 5) correlations present in these deviations from thermality have the capacity to carry off the maximum information content of the hole.

4.2 F→R tunneling: tunneling through the future horizon of an astrophysical black hole

In a real black hole formed by collapse, the L-sector of the L→R tunneling scenario does not exist. A picture that corresponds more closely to our intuitive idea of Hawking evaporation is shown in Figure 3. A virtual particle, represented by a thin or thick spherical shell (outer and inner face histories Σ_+ and Σ_-), formed just beneath the future horizon H^+ , tunnels through the horizon from sector F to sector R and escapes. The attendant loss of mass causes the horizon to shrink from H^+ to H^- . (In Figs 3(a) and (b) the two face histories Σ_+ and Σ_- are shown separately for clarity.)

Using this overall picture, we shall here derive two formulae for the tunneling probability $P(E)$, based on the thin- and thick-shell models, and follow up with a discussion. Both formulae appear in the literature, sometimes in one and the same paper. In the simplest case of Schwarzschild evaporation the two formulae are equivalent, but they differ in general.

For optimum tunneling probability, the outward pre-tunneling velocity should be as large, and post-tunneling velocity as small (compatible with marginal escape from the horizon) as possible. This requires that both pre- and post-tunneling histories should be very nearly surfaces of constant retarded time u . Tunneling thus takes place between two given values of u , inside and outside that horizon, where

$$u = -\frac{1}{\kappa_\epsilon} \ln U_\epsilon \quad (\epsilon = \pm)$$

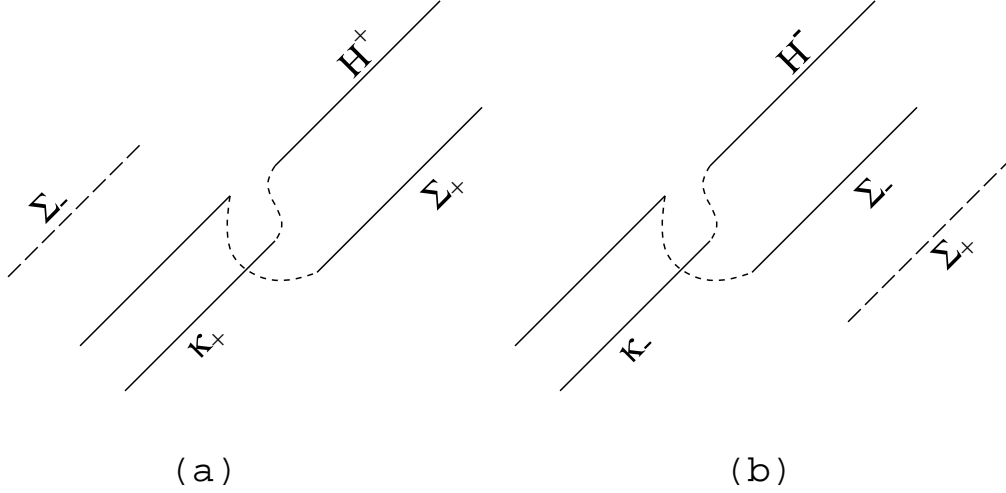


Figure 3: Shell-tunneling through the future horizon. First (a), the outer face Σ_+ tunnels through the initial location H^+ of the apparent horizon. Finally (b), the inner face Σ_- tunnels through the shrunk horizon H^- .

and κ_+ and κ_- are the surface gravities before and after the shell has escaped. According to (4.3), in the process $\text{Im } u$ jumps from $\frac{\pi}{2\kappa_+}$ before the horizon shrinks to $-\frac{\pi}{2\kappa_-}$ afterwards.

(One way to visualize the tunneling for a thin shell is to imagine the pre- and post-tunneling histories reslotted so that the $U_+ = 0$ and $U_- = 0$ axes are aligned. This permits both histories to be mapped onto a single Kruskal diagram.)

In the Appendix it is noted that Schwarzschild time t may be subjected to arbitrary space-dependent translations

$$t \rightarrow t_{gen} = t + \psi(r) \quad (4.10)$$

without affecting the validity of the expression for the Jacobi action

$$W = - \int M d\tau + \int dE \int dt_{gen}(E) \quad (4.11)$$

or the definition of conjugate variable E , the energy measured at infinity. (We have slightly extended the thin-shell expression (A.24) so as to be applicable also to thick shells with layers of energy dE – not an exact differential in general.) where, as in (4.5), the tunneling energy dE is given by the (inexact for $e \neq 0$) differential form

$$dE = dm - \frac{e}{r_H} de \quad (4.12)$$

For the tunneling episode, the natural choice of parameter is $t_{gen} = u$. This yields for the imaginary part of the thin-shell action

$$\text{Im } W_{thin} = E_{thin} \text{Im } \Delta u = E_{thin} \overline{\left(\frac{\pi}{\kappa} \right)} \quad (4.13)$$

and for a thick shell,

$$\text{Im } W_{thick} = \int dE \frac{\pi}{\kappa(E)} \quad (4.14)$$

where $\kappa(E)$ is the surface gravity after mass E has been lost by the hole. (Along the pre- and post- tunneling segments, one could take $t_{gen} = v$. They, of course, do not contribute to $\text{Im } W$.)

We can now go on to consider in turn the thin- and thick- shell tunneling models.

For a *thin shell*, we obtain from (4.5), and the work of the Appendix,

$$E_{thin} = - \left(\Delta m - \overline{\left(\frac{e}{r_H} \right)} \Delta e \right)$$

where $\Delta m, \Delta e$ are the (negative) changes in the hole's mass and charge.

This yields the tunneling probability

$$P_{thin}(E) = e^{-2\text{Im } W} = \exp \left(- \overline{\left(\frac{2\pi}{\kappa} \right)} E_{thin} \right), \quad (4.15)$$

in agreement with our result (4.9) for L→R thin-shell tunneling. We note that E_{thin} can be written more simply:

$$E_{thin} = -\Delta \left(m - \frac{1}{2} \frac{e^2}{r_+} \right) = -\frac{1}{2} \Delta r_+.$$

In the case of a *thick shell*, we are faced with the inexactness of dE when $e \neq 0$, which makes the line integral (4.14) path-dependent and non-unique. If, however, we assume further that the evaporation is, to a sufficient approximation, quasi-stationary – i.e., that we can neglect dissipative effects like gravitational radiation as the hole settles into its new configuration – then it follows from the first law of black hole mechanics [11] that

$$-2\pi dE/\kappa(E) = \frac{1}{4} dA = dS \quad (4.16)$$

the (negative) changes of horizon area and Bekenstein-Hawking entropy, which *are* exact differentials.

The integral (4.14) now gives exactly and unambiguously

$$P(\Delta m, \Delta e) = e^{\Delta S} \quad (4.17)$$

Because this derivation does not rely on spherical symmetry in any essential way, (4.17) extends readily to the evaporation of holes with spin. One then replaces (4.16) with the extended first law [11]

$$\frac{1}{4} dA = \frac{2\pi}{\kappa} (dm - \Phi_H de - \omega_H dJ) \quad (4.18)$$

where J is the hole's angular momentum and ω_H the angular velocity of the horizon. We forgo further details here, since the extension is straightforward. (In contrast, the corresponding

extension of the thin-shell formula(4.13) encounters the difficulty that it is generally impossible to achieve isometry of the two faces of a thin shell sandwiched between different Kerr geometries.)

In (4.15) and (4.17) we have two different formulae, based on a thin-shell and a continuum model respectively, for the emission probability P from a charged black hole. Explicitly, the exponents are

$$-\overline{\left(\frac{2\pi}{\kappa}\right)}E = \pi\overline{\left(\frac{r_H^2}{\sqrt{m^2 - e^2}}\right)}\Delta r_H, \quad \Delta S = 2\pi\overline{r_H}\Delta r_H \quad (4.19)$$

for the thin- and thick-shell cases respectively. For uncharged black holes these two expressions agree, but they begin to diverge for non-vanishing charge.

It will require a deeper investigation to decide which of these expressions is more correct, or (more likely) to bring to light some more complex formula which amalgamates features of both. Both depend only, as they should, on the observable, i.e. the states before and after emission.

One expects discontinuous aspects of the quantized emission to be more marked at low temperatures, and here the thin-shell formula (4.15), which predicts zero emission probability for zero temperature ($\kappa_+ = 0$), accords well with expectations. In general, however, it is not clear how well a thin-shell idealization is able to handle the complex form of the Einstein-Maxwell interaction term $ede/r_H(m, e)$ in (4.12). The arithmetic-mean prescription (A.17) for the thin-shell action was designed to deliver the right classical equations of motion (A.18) for the shell, but that depends on the simple bilinear form $q\varphi$ of the interaction (A.15). Arithmetic-mean recipes are generally limited to linear theories (like Einstein's in the distributional limit – only terms linear in second metric-derivatives survive in the curvature) and bilinear interactions. On these grounds we tend to favour the continuum-model formula (4.17) over (4.15) for charged black holes whose surface gravity is not too small. It is questionable whether naturally evaporating black holes ever approach a state of extremality (stable or unstable); numerical evidence suggests that angular momentum and charge are evaporated preferentially. All of this raises questions worth exploring further, in particular the speculative possibility of stable, information-storing black hole remnants.

5 Correlations, entropy, unitarity

We found in the previous section that the probability of a black hole of mass m and charge e (hence Bekenstein-Hawking entropy $S(m, e) = \frac{1}{4}A_H$) decaying to a state (m_1, e_1) is

$$P(m, e \rightarrow m_1, e_1) = e^{-(S-S_1)} \quad (5.1)$$

according to a thick-shell model for the evaporating particle. (On the alternative thin-shell model, (5.1) becomes an inequality, $P < e^{-(S-S_1)}$.) The result is obviously transitive and leads to

$$P(m, e \rightarrow m_1, e_1 \rightarrow m_2, e_2 \rightarrow \cdots \rightarrow 0) = e^{-S(m, e)}$$

for any chain of decays ending in complete evaporation. If $N(m, e)$ is the number of ways the hole can evaporate, we must have $NP = 1$. Hence

$$N = e^S \quad (5.2)$$

This gives an interpretation of the Bekenstein-Hawking entropy in terms of the number of modes of evaporation. Equation (5.1) can now be reinterpreted as equating, to leading order (up to a neglected cross-section factor), the transition probability to a statistical factor e^{S_1}/e^S , equal to the ratio of the number of final states to initial states.

Thus, the degrees of freedom in the outgoing radiation equal (or even exceed, on the thin-shell model) the maximum information capacity of the hole, as measured by the Bekenstein-Hawking entropy. This provides evidence, purely on the basis of counting, that unitarity could be preserved and that the radiation has enough room to accommodate all of the information. (But this has not been a matter of universal agreement[3].)

In a significant paper [4], Zhang et al have reopened the question whether deviations from exact thermality encoded in (4.15) or (5.1) produce correlations actually capable of carrying information.

Generally, one defines the correlation coefficient $C(a, b)$ between two events a and b by

$$C(a, b) = \ln \frac{P(a, b)}{P(a)P(b)} \quad (5.3)$$

where $P(a, b)$ is the probability of both a and b , and $P(b) = \sum_a P(a, b)$ the probability of b . The *conditional* probability of b (given that a has already occurred) is

$$P(b|a) = \frac{P(a, b)}{P(a)} \quad (5.4)$$

In our case (confining the argument to uncharged evaporation for simplicity), the probability that a black hole of mass m emits a quantum of energy E is, by (5.1),

$$P(m, E) = \exp \left\{ -4\pi[m^2 - (m - E)^2] \right\}$$

and this yields a nontrivial correlation [4]

$$C(E_1, E_2) = \ln \frac{P(m, E_1 + E_2)}{P(m, E_1)P(m, E_2)} = 8\pi E_1 E_2 \quad (5.5)$$

It might be thought that one should replace $P(m, E_2)$ in (5.5) by $P(m - E_1, E_2)$ to take account of mass loss from the first emission. That would be tantamount to replacing $P(b)$ in (5.3) by the conditional probability $P(b|a)$. But one sees at once from (5.4) that this would give $C(a, b) = 0$ identically for *any* two events. The argument is clearly circular: it absorbs the correlations themselves into the test for their existence.

Thus, as emphasized in [4], the original conclusion (5.5) is correct. The radiation does have correlations and, according to (5.2), these have the capacity to carry off the maximum information content of the hole.

6 Summary and conclusions.

The argument for information loss in black hole evaporation rested, first and foremost, on the belief that the emerging spectrum is exactly thermal. Since 1994 this main pillar of the argument has toppled. A series of investigations has shown that, when back-reaction of the emission is allowed for, there are departures from thermality[2], and that the associated correlations have the capacity to carry off the maximum information content of the hole [4]. In this paper we have reviewed, simplified and somewhat extended this work.

A logically prior issue, not touched on in this work, is the extent to which the emission process can access and extricate information buried in the depths of the hole. The wavelength and period of the radiation when it reaches infinity are of the order of the hole's diameter and characteristic internal time (i.e. maximum proper free-fall time from the horizon), suggesting that access is possible. On the other hand, the original mode analyses, (non-local, but still the best evidence for thermality across the spectrum) and the usual particle tunneling and pair-creation arguments suggest a localized, near-horizon process with high frequencies at formation that are subsequently redshifted. This would make the emission an exclusively surface process, without access to the interior. However, the uncertainty principle forbids such definite allocation of the place and time of emission for a quantum of given energy. It cannot be ruled out that much of the radiation reaches infinity without substantial redshift, having been formed by concerted, coherent action of the entire hole. The issue clearly needs further study (cf [12]) but may well turn out to be a red herring as a possible culprit for information loss.

Steve Carlip kindly informs us that equation (4.17) was previously obtained by Massar and Parentani [13], using path-integral methods developed by Carlip and Teitelboim.

We thank Samir Mathur, Douglas Singleton and the referee for correspondence and helpful suggestions.

A Review of shell dynamics

This appendix collects and reviews the origins of the shell formulae used in section 4. More detail can be found in chapter 3 of Poisson's *Toolkit* [7].

The shell history is a timelike 3-space Σ that divides spacetime into two sectors \mathcal{V}_+ and \mathcal{V}_- mapped by independent charts x_+^α and x_-^α and with metrics

$$ds_\pm^2 = g_{\alpha\beta} dx^\alpha dx^\beta|_\pm$$

(Greek indices run from 1 to 4). Their common boundary Σ is described by two sets of imbedding relations $x_\pm^\alpha = x_\pm^\alpha(\xi^a)$ and intrinsic 3-metric

$$ds^2 = g_{ab}(\xi) d\xi^a d\xi^b$$

in terms of a third independent set of intrinsic coordinates ξ^a (Latin indices run from 1 to 3). The intrinsic 3-metric g_{ab} is induced compatibly on Σ by each of the two 4-geometries

via

$$g_{ab}(\xi) = \left(g_{\alpha\beta}(x) e_{(a)}^\alpha e_{(b)}^\beta \right)_\pm, \quad e_{(a)}^\alpha(\xi)|_\pm = \frac{\partial x_\pm^\alpha}{\partial \xi^a} \quad (\text{A.1})$$

where $e_{(a)}$ are three basis vectors tangent to Σ .

The interior and exterior imbeddings $(ds)_{\Sigma_+}^2 = (ds)_{\Sigma_-}^2$ thus induce a unique tangential 3-metric g_{ab} on Σ ; However, its extrinsic curvatures

$$K_{ab}^\pm = n_{\alpha| \beta} e_{(a)}^\alpha e_{(b)}^\beta |^\pm \quad (\text{A.2})$$

in \mathcal{V}_+ and \mathcal{V}_- will generally differ in the presence of a shell of matter. (Here, n_α is the unit spacelike normal, directed from \mathcal{V}_- to \mathcal{V}_+ and the stroke denotes 4-dimensional covariant differentiation; 3-dimensional covariant derivatives with respect to g_{ab} are indicated by a semi-colon)

The jump of extrinsic curvature across Σ ,

$$[K_{ab}] \equiv K_{ab}^+ - K_{ab}^-$$

gives the shell's intrinsic stress-energy tensor S_{ab} via a surface analogue of Einstein's field equations:

$$-8\pi S_{ab} = [K_{ab} - g_{ab}K] \quad (\text{A.3a})$$

$$S^b_{a;b} = -[e_{(a)}^\alpha T_\alpha^\beta n_\beta] \quad (\text{A.3b})$$

Equation (A.3b) is an energy conservation law, describing the shell's response to the stresses and energy fluxes in its surroundings.

Variation of the metric in the action

$$I = I_{geom} + I_{mat}$$

where

$$16\pi I_{geom} = \int_{bulk} d^4x \sqrt{-g} R_\alpha^\alpha - 2 \int_\Sigma [K] d\Sigma \quad (\text{A.4})$$

yields, beside Einstein's field equations, also the jump conditions (A.3a) Here, the shell is treated simply as an isometric pair of timelike boundaries Σ_+ and Σ_- of the bulk, with a common normal n , directed from \mathcal{V}_- to \mathcal{V}_+ .

The key geometrical result needed in the derivation is that the variation of

$$I = \int_{bulk} d^4x \sqrt{-g} R_\alpha^\alpha + \int_{boundary} 2\epsilon K d\Sigma \quad (\text{A.5})$$

is

$$\delta I = \int_{bulk} G^{\alpha\beta} \delta g_{\alpha\beta} \sqrt{-g} d^4x + \int_{boundary} \pi^{ab} \delta g_{ab} d\Sigma \quad (\text{A.6})$$

where $\pi_{ab} = -\epsilon(K_{ab} - g_{ab}K)$, $\epsilon = n \cdot n = \pm 1$ and n is now the outward normal to the bulk, bounded by a timelike or spacelike Σ . An apparent sign discordance between (A.4) and (A.5) merely reflects these differing conventions for the orientation of n .

Variation of the material part of the action I_{mat} gives the stress-energy tensor of the shell and its environment according to

$$\delta I_{mat} = \int \frac{1}{2} T^{\alpha\beta} \delta g_{\alpha\beta} \sqrt{-g} d^4x + \int \frac{1}{2} S^{ab} \delta g_{ab} d\Sigma \quad (\text{A.7})$$

Vanishing of (A.6)+(A.7) gives the Einstein field equations $G^{\alpha\beta} = 8\pi T^{\alpha\beta}$ and the shell equation (A.3a).

For a shell of fluid in a fluid environment, I_{mat} takes the form

$$I_{mat} = - \int_{bulk} \rho(n, s) \sqrt{-g} d^4x - \int_{\Sigma} \sigma(n, s) d\Sigma \quad (\text{A.8})$$

where ρ and σ are energy densities per unit volume and unit area respectively, and s, n the corresponding entropy and molecular number densities. (Our use of the same symbols n, s for densities per unit volume and unit area in these different contexts should not cause confusion.)

Our specific concern in section 4 is with a class of spherical shells moving in spherical geometries of the form

$$(ds^2)_{\pm} = \frac{dr^2}{f(r)} + r^2 d\Omega^2 - f(r) dt^2 \quad (\text{A.9})$$

with different functions f_- and f_+ and time coordinates t_- and t_+ in \mathcal{V}_- and \mathcal{V}_+ . In all geometries of the form (A.9), the Einstein field equations require $T_r^r = T_t^t$, which implies that $e_{(a)}^{\alpha} T_{\alpha}^{\beta} n_{\beta} = 0$ and $S_{a;b}^b = 0$ at the shell by virtue of (A.3b). Thus in this class of spacetimes, the ambient pressures do no work and the shell's internal energy is conserved.

The junction and conservation laws (A.3) now reduce to a single equation of motion for the shell radius $R(\tau)$:

$$[\mathcal{E}] = -\frac{M}{R} \quad (\text{A.10a})$$

$$dM + Pd(4\pi R^2) = 0 \quad (\text{A.10b})$$

where $M = 4\pi R^2 \sigma$ is the shell's proper mass, $\sigma = -S_{\tau}^{\tau}$ and $P = S_{\theta}^{\theta} = S_{\phi}^{\phi}$ is the surface pressure. The expression (A.10a) follows at once from

$$K_{\theta}^{\theta} = \frac{1}{2} n^{\alpha} \partial_{\alpha} \ln g_{\theta\theta} = n^r / R = \mathcal{E} / R \quad (\pm \text{understood})$$

where

$$\mathcal{E} = n \cdot \nabla r = \eta \sqrt{f + R_{\tau}^2} \quad (\text{A.11})$$

The sign factor $\eta = \pm 1$ determines whether r is increasing or decreasing outwards (i.e, in the direction from \mathcal{V}_- to \mathcal{V}_+), and the subscript τ indicates $\frac{d}{d\tau}$. (Physically, \mathcal{E}_- and \mathcal{E}_+ could be interpreted as energies of test particles of unit rest mass attached to the inner and outer shell faces.)

The rationalized version of (A.10a) is

$$R_{\tau}^2 = \left(\frac{m_{\Sigma}}{M}\right)^2 - \bar{f}(R) + \frac{1}{4} \left(\frac{M}{R}\right)^2 \quad (\text{A.12})$$

The bar denotes an arithmetical mean $\bar{f} = \frac{1}{2}(f_+ + f_-)$ and we have defined the Schwarzschild mass $m(r)$ interior to radius r by

$$f(r) = 1 - \frac{2m(r)}{r}, \quad m_\Sigma = m_+(R) - m_-(R)$$

The simplest illustration is a shell of mass m in empty space: (A.10) or (A.12) yields

$$m = M\sqrt{1 + R_\tau^2} - \frac{M^2}{2R}$$

which is a decomposition of the total (conserved) mass-energy m in a form whose Newtonian counterpart is self-evident.

These results extend readily to charged shells. We simply augment the action (A.4)+(A.8) with an interaction term

$$I_{int} = \int J^\alpha A_\alpha \sqrt{-g} d^4x \quad (\text{A.13})$$

plus the usual free-field Lagrangian $-\frac{1}{16\pi}F_{\alpha\beta}F^{\alpha\beta}$. Our spherical constraint admits only radial electric fields, for which A_α is gauge-reducible in static (r, t) coordinates to a single component

$$A_t = -\varphi = -\frac{e_\pm}{r} \quad (\text{A.14})$$

in \mathcal{V}_\pm respectively, up to an additive constant which could be adjusted across the shell. The shell's charge is $q = e_+ - e_-$ and (A.13) reduces to

$$I_{int} = \int q A_\alpha dx^\alpha \quad (\text{A.15})$$

Adding (A.15) to the action does not affect the junction conditions or equations of motion in the forms (A.3), (A.10) or (A.12). (They were obtained by varying the metric in the action; however, (A.15) is independent of the metric.) Electric forces are nonetheless now at work in these equations, for instance through the Faraday stresses now present in T_α^β on the right-hand side of (A.3b).

Our assumption of spherical symmetry has reduced the effective dynamics to one degree of freedom – the shell radius R . We recall that the shell was introduced in the first place in Sec. 4 as an s-wave approximation to the wave function for *particles* tunneling radially, so that a (1+1)-dimensional description is entirely apposite. However, the action that we have is still (3+1) dimensional, and saddled with elements, such as a 3-dimensional extrinsic curvature, foreign to a (1+1)-dimensional dynamics. It is therefore appropriate to seek a (1+1)-dimensional effective Lagrangian which delivers the same equations of motion for R and whose Hamiltonian generates the corresponding quantum evolution.

A Lagrangian of this sort emerges if we retain just the mechanical, non-geometrical parts (A.8)+(A.13) of the original action:

$$I_{eff} = - \int M d\tau + \int q A_\alpha dx^\alpha \quad (\text{A.16})$$

To fix the Lagrangian we still need to choose a time-coordinate invariant under Euler-Lagrange variation of the particle's world-line. (Proper time τ (=arc length) is clearly inadmissible) As we shall see, a formally successful (as well as physically desirable) choice is a static observer's time t , split evenly between the alternatives t_+ and t_- by taking the arithmetic mean of the $+$ and $-$ actions. This prescription leads to the following explicit form of (A.16):

$$I_{eff} = \int \overline{L} dt, \quad L = -M \frac{f}{\mathcal{E}} - q\varphi \quad (\text{A.17})$$

The upper bar denotes an arithmetic mean, $\overline{X} \equiv \frac{1}{2}(X_+ + X_-)$; $\varphi_{\pm} = e_{\pm}/R - c_{\pm}$, where c_{\pm} are adjustable constants, and we have used $d\tau = (f dt/\mathcal{E})_{\pm}$, which follows from (A.11).

The Euler-Lagrange equation $\delta I_{eff}/\delta R = 0$ for (A.17) gives

$$R_{\tau\tau} \left(\frac{1}{\mathcal{E}} \right) + \frac{1}{2} \left(\frac{f'(R)}{\mathcal{E}} \right) + \frac{\overline{\mathcal{E}}}{M} \frac{dM}{dR} - \frac{q}{MR^2} \overline{e} = 0 \quad (\text{A.18})$$

Where prime indicates that it is a differentiation with respect to R .

On the other hand, the junction condition (A.10a) can be written in either of the forms ($\epsilon = \pm$)

$$\frac{2M}{R} \mathcal{E}_{\epsilon} = f_- - f_+ - \epsilon \frac{M^2}{R^2} \quad (\text{A.19})$$

Addition yields

$$\frac{2M}{R} \overline{\mathcal{E}} = f_- - f_+ \quad (\text{A.20})$$

Differentiation of this equation yields a second order equation of motion identical with (A.18), when f has the Reissner-Nordström form.

Thus (A.17) is indeed the desired *effective particle action* for the shell.

The canonical radial momentum and Hamiltonian associated with Lagrangian (A.17) are

$$\begin{aligned} p_r &= \frac{\partial L}{\partial R_t} = \frac{M}{f} R_{\tau} \\ H &= p_r R_t - L = M\mathcal{E} + q\varphi \end{aligned} \quad (\text{A.21})$$

\overline{H} is conserved by Hamilton's equations for a time-independent background. Explicit evaluation for Reissner-Nordström fields, using definition (A.11), shows that

$$\overline{H} \equiv E = m - \overline{c} \quad (\text{A.22})$$

where $m = m_+ - m_-$, $\overline{c} = q\overline{e}/r_H$ equal to the shell's Schwarzschild mass. It is, incidentally, straightforward to verify that (A.16) is the action, and (A.21) the Hamiltonian, for a charged test *particle* moving radially in the spherical geometry (A.9).

The effective action (A.17) is taken between given endpoints (R_i, t_i) ($i = 1, 2$). Under a change of endpoints, the change of extremal action is given by the Hamilton-Jacobi formula

$$\delta I_{eff} = [\overline{p} \delta R - \overline{H} \delta t]_1^2 = [p \delta R] - E(\delta t_2 - \delta t_1) \quad (\text{A.23})$$

(where we have assumed $\delta t_+ = \delta t_-$)

Our interest in section 3 et seq is in the probability for a particle of given *energy* E to tunnel between given points R_1 and R_2 straddling a horizon; the tunneling time is irrelevant. The path which maximizes this probability is the path which minimizes the Jacobi action.

$$W \equiv I_{eff} + \int E dt \quad (\text{A.24})$$

for which (A.23) gives

$$\delta W = [p\delta R + t\delta E] = [p\delta R] + (t_2 - t_1)\delta E \quad (\text{A.25})$$

As is evident from this form of the Hamilton-Jacobi formula, the Hamiltonian, and hence also the Jacobi action (A.24) (with the same energy E) are invariant under space-dependent translations of the time coordinate. Thus, (A.24) remains valid if t is replaced, for example, by retarded or advanced times u, v (See (4.1)), or by any of a class of generalized times t_{gen} , defined by

$$dt_{gen} = dt \pm \alpha(f) \frac{dr}{f},$$

in which α has an arbitrary dependence on $f(r)$ subject to $\alpha(0) = 1$. That includes Painlevé-Gullstrand time, defined by

$$dt_{PG} = dt + \sqrt{1 - f} \frac{dr}{f},$$

References

- [1] Sabine Hossenfelder and Lee Smolin, gr-qc/0901 3156
Samir D. Mathur, hep-th/0803 2030, hep-th/0909 1038, hep-th/1012 2101
- [2] P. Kraus and F. Wilczek, Nucl. Phys. B433, 403 (1995)
P. Kraus and. F. Wilczek, Nucl. Phys. B437, 231 (1995)
M. K. Parikh, F. Wilczek, Phys. Rev. Lett. 85, 5042(2000) (hep-th/9907001)
- [3] Maulik K. Parikh hep-th/0402166, hep-th/0405160
M.K. Parikh, Int. J. Mod. Phys. D13, 2351 (2004)
M. Arzano, A. Medved and E. Vagenas, J. High Energy Phys. 0509 (2005) 037 ;
hep-th/0505266
- [4] B. Zhang, Q.y. Cai, L. You and M.S. Zhan, Phys. Lett. B98 675 (2009) (hep-th/0906 5033); hep-th/0903 0893
- [5] J. Schwinger, Phys. Rev. 82, 664 (1951)
V. S. Popov, Sov. Phys. JETP 34, 709 (1972)
R. Brout, S. Massar, R. Parentani, and Ph. Spindel, Phys. Rep. 260, 329 (1995) gr-qc/0710 4345
K. Srinivasan, T. Padmanabhan, gr-qc/9812087

- [6] Richard P. Feynman and A. R. Hibbs, Quantum Mechanics and Path Integrals, (McGraw-Hill, New York) 1965
- [7] Eric Poisson, A Relativist's Toolkit: The Mathematics of Black-Hole Mechanics, Cambridge University Press, 2004
- [8] Rafael D. Sorkin, gr-qc/0911 1479
Steven B. Giddings gr-qc/0911 3395
- [9] Landau, L. D. and Lifschitz, E. M, Quantum Mechanics (Pergamon Press, 1975) Chaps 3 and 7.
K. Srinivasan, T. Padmanabhan, gr-qc/9807064
- [10] P. Kraus and F. Wilczek, Nucl. Phys. B 437,231 (1995); gr-qc/9408003.
- [11] R. M. Wald, General Relativity p.336 (University Of Chicago Press, Chicago 1984)
- [12] R. Schützhold and W. G. Unruh, Phys. Rev. D 78, 041504 (2008), gr-qc/0804 1686
- [13] S.Massar and R.Parentani, Nucl.Phys. B575,333(2003); gr-qc/9903027